"Physics of Auroral Phenomena", Proc. XXVI Annual Seminar, Apatity, pp. 53-56, 2003

Polar Geophysical Institute

LUMINOSITY INTENSITY OF DIFFERENT TYPE AURORAS VERSUS GEOMAGNETIC ACTIVITY

L.S. Yevlashin, Yu.P. Maltsev *(Polar Geophysical Institute, Apatity)*

Abstract. Analysis of auroral luminosity in the visible part of the spectrum is performed for three types of auroras: proton auroras, electron auroras and the red type A ones under various geomagnetic conditions. It is found that for the same value of Kp-index, the integral intensity of the luminosity for the auroras excited by precipitating electrons is on average 1.5-2 times greater than that for the auroras associated with precipitating protons. The spatial and temporal distribution of proton and electron auroras mapped to the ionosphere represents two intersecting branches. In the evening hours proton auroras are statistically observed equatorward of electron ones. In the morning sector the situation is opposite. Around midnight the band of electron precipitation is continuous, whereas that of the proton precipitation is disrupted. Using magnetic measurements of Dynamic Explorer 2 satellite, the distribution of the field-aligned currents (FACs) under moderate disturbance is built up. The regions of proton and electron precipitation are statistically coincident with the regions of both upward and downward FACs. This suggests that the precipitating particles contribute significantly to the FACs.

1. Introduction

The problem of energy dissipation during magnetospheric storms has been considered by many authors. In particular, Akasofu [1981] assumed that a noticeable part of the energy is spent on formation of the ring current, ionospheric heating by the electric currents, and dissipation in the ionosphere related to precipitating particles. This latter part provides extra heating of the upper atmosphere (~60%), a certain ionization level (~10%), and auroral emissions over the whole spectrum (30%) [Rees, 1975]. The problem of emission energy spectral distribution is highly debating. As for the visible part of the spectrum, the value of 5% of the total dissipation energy in the ionosphere related to the precipitating particles is thought to be a reasonable assessment. However, it is quite possible that this energy is redistributed over the luminosity spectrum depending on the type of aurora, e.g. proton auroras, electron auroras and red type A auroras.

Satellite observations of precipitating particles indicate that typically proton and electron fluxes are registered simultaneously, however, the ratio of flux intensities may vary considerably depending on precipitation region and MLT (see, e.g. [Hardy et al., 1989]) and cause auroral luminosity of different types. The data on the reciprocal position of luminosity regions related to protons and electrons are somewhat conflicting. According to a number of studies, proton auroras are always located equatorward of the electron ones (e.g. Eather and Sandford, [1966]; Akasofu, [1968]). Other authors claim that there are two intersecting branches of luminosity related to precipitating protons and electrons, respectively. In the evening, the proton branch is located equatorward of the electron one, and vice versa in the morning hours [e.g. Wiens and Vallance Jones, 1969; Yevlashin, 1970].

The purpose of this paper is to estimate the luminosity energy in the visible part of the spectrum for the proton, electron and red type A auroras in order to outline the major regions of auroral particle precipitation. Besides, we mean to clarify the relation between magnetospheric field-aligned currents and precipitation regions connected with certain types of auroras.

2. Data

The data to be processed had been obtained with the C-180-S spectral camera at observatories Murmansk and Loparskaya in the period from 1957 to 1991. The integral intensity of auroral luminosity was determined as a sum of major emissions: $\Sigma\ I_{687.5} + I_{678.8} + I_{670.4} + I_{656.3} + I_{557.7} + I_{630.0} + I_{636.4} + I_{391.4} + I_{427.8} + I_{470.9} + I_{cont.}$ In order to determine the intensity of the emissions, which had not been measured, the following ratios were adopted: $I_{391.4} : I_{427.8} : I_{470.9} = 9:3:1$; $I_{630.0} : I_{636.4} = 3:1$ [Chamberlain, 1961].

According to [Yevlashin, 1970], the intensity of hydrogen emission Hα λ 656.3 nm was set by the four point scale: 1 – I = 0.3 kR; 2 - I = 0.6 kR; 3 – I = 1 kR; 4 – I $\geq$ 2 kR. The intensity of the continuum according to the above scale for all visible spectrum was supposed to be constant and equal to: 1 = 10 R/nm; 2 = 20 R/nm; 3 = 30 R/nm; 4 = 40 R/nm.

In order to reproduce the field-aligned currents we used Dynamic Explorer-2 magnetic measurements, taken for 1.5-year period from August 1981 to February 1983. The satellite had a polar orbit at the height of ~ 700 km.

3. Results

3.1. Auroras

The types of auroras to be studied were chosen, considering their spectral characteristics. Thus proton auroras selected, were those caused by precipitating protons with energies from 1 to 100 keV (the average value ~20 keV), with the intensity of H_α λ 656.3 nm hydrogen emission in their spectra exceeding 0.1 of the green oxygen line [OI] λ 557.7 nm intensity [Eather, 1967]. These were mostly diffuse forms (arcs, diffuse structures) with not more than 2 points of brightness (by IBC scale). To estimate the summarized intensity of proton aurora emissions we chose the observations, dating back to the period of very high solar activity: International Geophysical Year (IGY)- International Geophysical Cooperation (IGC) (1957-1960).

There were taken three observational seasons: 1957-1958, 1958-1959 and 1959-1960 and 139 nights when weather and light conditions allowed for observations of hydrogen emission H_α λ 656.3 nm. Since during the night the intensity of hydrogen emission could vary, each night was characterized by the intensity maximum as well as by the maximum through the night Kp value. Then, the total intensity over the spectrum was calculated. It is presented in Fig.1a versus Kp-index, kilorayleighs being reduced to erg/cm^2 sec.

We treated the electron auroras, in whose spectra the intensity of the hydrogen emission Hα did not exceed 0.2 kR, whereas 1PGN_2 bands (in particular, λ 687.5 nm; 678.8 nm; 670.4 nm) amounted to a few dozen kilorayleighs, depending on the green line λ 557.7 nm intensity. Those were mainly bright auroras, having ray structure, of green, sometimes with red lower edge (red auroras of type B). Such auroras are produced by auroral electrons with energies from 1 to 30 keV [Chamberlain, 1961].

To determine the total intensity of the electron aurora emissions versus Kp-index, we chose one more period of high solar activity, that is International Magnetosphere Research (IMR) interval, and used, in sum, 30 nights (see Fig.1b).

Red auroras of A type are those perceived red by disarmed eye (arcs, diffuse structures, spots, rays, etc.), in which spectra the intensity of the red oxygen emission [01] λ 630.0 nm exceeds 10 kR, with the ratio of intensities $I_{630.0}$ and $I_{577.7}$ being greater than 2. Presumably, the source of such auroras are electrons with energy < 1 keV [Chamberlain, 1961].

For statistical study of spectral characteristics of the red type A auroras a long period of observations from 1957 to 1991 was used, as auroras of this type are rather scare even in the auroral zone. In sum 42 nights, when red auroras were registered using C-180-S at obs. Murmansk and Loparskaya, were selected. The resulting dependence of the total intensity of the aurora emissions on Kp-index is shown in Fig. 1c.

From comparing Figs 1a, 1b, and 1c, we can see that the most intensive auroras in the visible part of the spectrum under close values of Kp-index are electron ones.

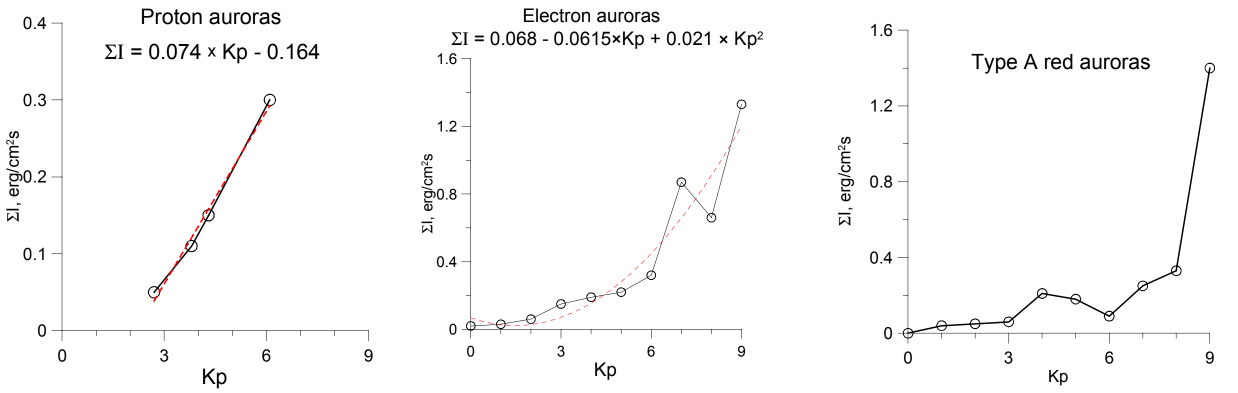

A b c

Fig. 1. Total intensity of emissions versus Kp in (a) the proton auroras, (b) electron auroras, and (c) type A red auroras. The dashed lines show the approximations.

Having assumed that the proton auroras are associated with the hydrogen emission Hα, while the electron ones with 1PGN_2 emissions, we analyzed the relationship between proton and electron auroras. There were built circle diagrams (Figs 2a, b), presenting distribution of the intensities of the emission Hα 656.3 nm and bands (5-2) 1PGN_2 λ 670.4 nm over geomagnetic latitude (60^0 – 70^0) and magnetic local time (MLT). Such diagrams were reproduced for different geomagnetic disturbance level (Kp = 0 – 5), both under high and low solar activity (seasons of 1981-1982 and 1985-1986, respectively). From comparison of the corresponding diagrams it follows that statistically in the evening sector the luminosity in the Hα 656.3 nm emission is located equatorward of the luminosity band of the λ 670.4 nm emission. In the morning sector the relative positions are opposite. This tendency is better pronounced in the period of high solar activity and strong magnetic disturbances. Such picture agrees well with the previous studies [Yevlashin, 1970] and statistical data on precipitations of protons and electrons obtained by DMSP spacecraft [Hardy et al., 1989].

3.2. Field-aligned currents

It is interesting to compare spatial distributions of different types of auroras and of the FACs. We have processed magnetic measurements of Dynamic Explorer-2 spacecraft performed in the period of 1.5 year. Horizontal magnetic disturbances under Kp = 5 were averaged in bins with the size of 1 degree of invariant latitude and 2 hours of local time. Then, using the formula

Auroras (intensity in R)

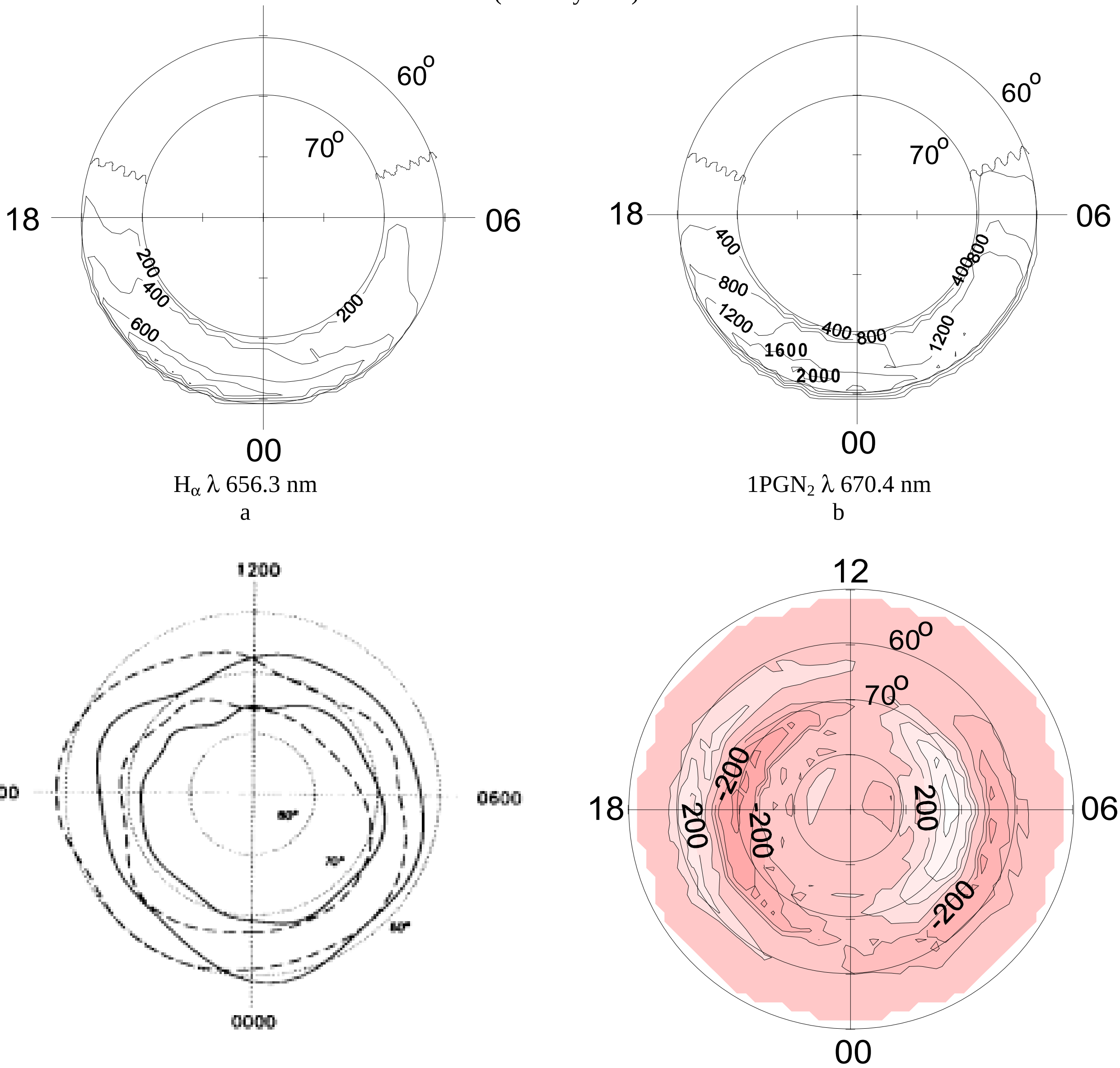

H_α λ 656.3 nm
a

1PGN$_2$ λ 670.4 nm
b

________ electrons
----------- protons
c

Field-aligned currents (in mA/km^2)
d

Fig. 2. Distribution of auroras and field-aligned currents under Kp = 5.
a) intensity of the proton auroras,
b) intensity of the electron auroras,
c) mutual location of electron and proton precipitation areas according to DMSP data,
d) field-aligned current density according to DE2 data.

$$j_z = \frac{1}{\mu_0}\left(\frac{\partial B_y}{\partial x} - \frac{\partial B_x}{\partial y}\right)$$

we calculated the vertical currents, which are nearly coincident with the field-aligned ones. Because of large scattering, the results were additionally averaged over 6 hours with the use of sliding average technique. The resulting distribution of the FACs is shown in Fig. 2d. One can see two zones of FACs. In the morning the downward currents are located poleward from the upward ones, while in the evening they are displaced more to the equator.

If we relate the downward currents mostly to precipitating protons and the upward ones to precipitating electrons, then the pattern of the downward (upward) FACs agrees with the distribution of proton (electron) precipitation shown in Fig. 2c.

4. Discussion and conclusions

In this study we have analyzed data on auroral luminosity in the visible part of spectrum for three types of aurora, i.e. proton auroras, electron auroras and the red type A ones, obtained at Murmansk and Loparskaya observatories with the C-180-S patrol spectrograph during 1957-1991 versus the Kp-index. The total intensity of the luminosity was estimated as a sum of separate emissions. We found that, for the same Kp value, the integral intensity of luminosity at the excitation of auroras by auroral electrons is on average 1,5 - 2 times larger compared to the excitation by auroral protons.

The spatial-temporal distribution of proton and electron auroras when mapped to the ionosphere is seen to consist of two intersecting branches. In the evening, proton auroras are statistically observed equatorward of the electron ones, while the opposite is true for morning hours (Figs 2a, b). This pattern corresponds to the one previously reported in [Yevlashin, 1970; Yevlashina, 1981] where it is noted that the band of electron auroras is continuous around midnight, while the band of proton auroras is disrupted. The bands of the FACs behave in a similar way (Fig. 2d; also see the paper [Iijima and Potemra, 1976]). The band of the upward current in the night sector is almost continuous, whereas the downward currents are disrupted near midnight.

The spatial distribution of proton and electron precipitation regions on the whole agrees with the pattern of electron and proton precipitation obtained in the papers [Hardy et al., 1989; Basu et.al., 1993], although one can hardly see any disruption of the proton precipitation band in the night sector.

It is often suggested that electrons are the carriers of both upward and downward currents, that is the upward current is carried by energetic (1 - 10 keV) electrons, whereas the downward current is transported by cold ionospheric electrons going into the magnetosphere. To assess the electric current transported by precipitating protons we will use the measurements of differential energetic spectrum by the SCATHA satellite from [Hardy et al., 1989] for Kp = 5. The total flux integrated over the energies from 150 eV to 100 keV is equal to 1.32×10^7 cm^{-2} s^{-1} sr^{-1}. If the pitch-angle distribution is isotropic, we find the downward flux through multiplying this value by π, which yields 4.13×10^7 cm^{-2} s^{-1}. Having multiplied this quantity by the proton charge, we will get the density of the field-aligned current of about 66 mA/km^2. The data of the DE2 satellite suggest that at Kp = 5 the maximum current density is ~400 mA/km^2 (Fig. 2d). In the night sector, according to the measurements of proton flux by SCATHA satellite, this density appears factor 2 smaller, i.e. 200 mA/km^2. Thus, on the average auroral protons provide about 30% of the field-aligned current.

Acknowledgments. This work was supported by the RFBR (grant 03-05-65379) and by the Department of physical science of the Russian Academy of sciences (program DPS-16). The authors are grateful to J. King and N. Papitashvili) for the data by Dynamic Explorer-2 satellite.

References

Akasofu S.-I. Polar and magnetospheric substorms // D.Reidel publishing company. 316 p. 1968.

Akasofu S.-I. Energy coupling between solar wind and the magnetosphere // Space Sci. Rev. V.28. N 2. P. 121-190. 1981.

Basu B., Jasperse, Stricland D.J., Daniell, Jr. Transport – theoretic model for the electron-proton-hydrogen atom aurora. 1. Theory // J.Geophys.Res. v.98. N 12A. P. 21517-21532. 1993.

Chamberlain J.W. Physics of the auroral and airglow // Academic Press. 777 p. 1961.

Eather R.H. Auroral proton precipitation and hydrogen emissions // Rev. of Geophys. V.5. N 3. P. 207-285. 1967.

Eather R.H. and Sandford B.P. The zone of hydrogen emission in the night sky // Austral. J.Phys. V.19. P. 25-33. 1966.

Hardy D.A., Gussenhoven M.S. and Brautigam D.A. Statistical model of auroral ion precipitation // J.Geophys.Res. V.94. N A1. P. 370-392. 1989.

Iijima T. and Potemra T.A. The amplitude distribution of field-aligned currents at northern high latitudes observed by Triad // J.Geophys.Res. V.81. N 13. P. 2165-2174. 1976.

Rees M.H. Magnetospheric substorms energy dissipation in the atmosphere // Planet.Space Sci. V.23. N 12. P.15-89-1596. 1975.

Wiens R.H. and Vallance Jones A. Studies of auroral hydrogen emission in west-central Canada. III. Proton and electron auroral ovals. Canad.J.Phys. V.47. N 14. P. 1493-1498. 1969.

Yevlashin L.S. Monochromatic of the patrol spectrograph in Murmansk // "Aurora". M. N 19. P. 12-26. 1970.

Yevlashin L.S., Yevlashina L.M. On the problem of space-time distribution of aurora glow // "Aurora and Airglow". M. N 28. P. 24-27. 1981.